Electronic Supplementary Material (ESI) for Catalysis Science & Technology.

Supporting Information

Ni/NiM_2O_4 (M = Mn or Fe) Supported on N-Doped Carbon Nanotubes as Trifunctional Electrocatalysts for ORR, OER and HER

Qing Qin, Lulu Chen, Tao Wei, Yimeng Wang and Xien Liu*

Key Laboratory of Eco-chemical Engineering, College of Chemistry and Molecular Engineering, Qingdao University of Science and Technology, Qingdao 266042, P. R. China

E-mail: liuxien@qust.edu.cn

Electrochemical measurements

Hydrogen evolution reaction (HER). The HER activities of the prepared catalysts were tested in a typical tri-electrode system with a carbon rod counter electrode and a reversible hydrogen reference electrode. The Ni foam (1 × 1 cm^2) coated with the catalyst was used as working electrode. 1 M KOH was used as the electrolyte. All LSV curves were obtained at a scan rate of 10 mV s^{-1} without iR compensation.

The preparation method of the working electrode was according to the following steps: First, 2 mg of catalyst and 40 μL of Nafion were added into 0.3 mL of a mixture of ultrapure water and ethanol (V_{water} : $V_{ethanol}$ = 1 : 2). The homogeneous catalyst ink was obtained by ultrasonicating for 20 min. Then, 35 μL of the catalyst ink was dropped onto the Ni foam and dried naturally.

Oxygen evolution reaction (OER). The OER performance of the two catalysts and the references was measured in a conventional three-electrode setup. The Ni foam (1 × 1 cm^2) modified with catalyst (0.21 mg cm^{-2}) was used as working electrode, a reversible hydrogen electrode and a carbon rod were used as reference electrode and counter electrode, respectively. The electrolyte was 1 M KOH solution. The scan rate for all the LSV curves was 10 mV s^{-1}.

Oxygen reduction reaction (ORR). The ORR activity of the catalyst was investigated by the RDE technique in O_2-satured 0.1 M KOH solution. The Hg/HgO electrode was used as the reference electrode and Pt wire was used as the counter electrode, respectively. All the LSV curves were obtained at a scan rate of 10 mV s^{-1}. All the potentials were versus to reversible hydrogen electrode (RHE) through RHE

calibration, according to the formula E (RHE) = E (Hg/HgO) + 0.0591pH + 0.098.

Zn-air batteries. Coating PTFE and the activated charcoal (the weight ratio = 3 : 7) on a nickel foam was used as the air cathodes. Each air cathode was fixed to ~ 700 μm in thickness. 200 μL of the Nafion and 10 mg of the catalyst was dispersed in 0.25 mL of ethanol and ultrasonicated to form a homogeneous ink. The catalyst ink of 200 μL was dropped into the above cathode and the air-cathode was put in a vacuum container. Thirty minutes later, a mildly pressing procedure was performed on the air-cathode. The prepared air-cathode was used for assembling primary Zn-air batteries. 6 M KOH was used as the electrolyte. Zn plate was used as the anode and Ni foam was used as the current collector.

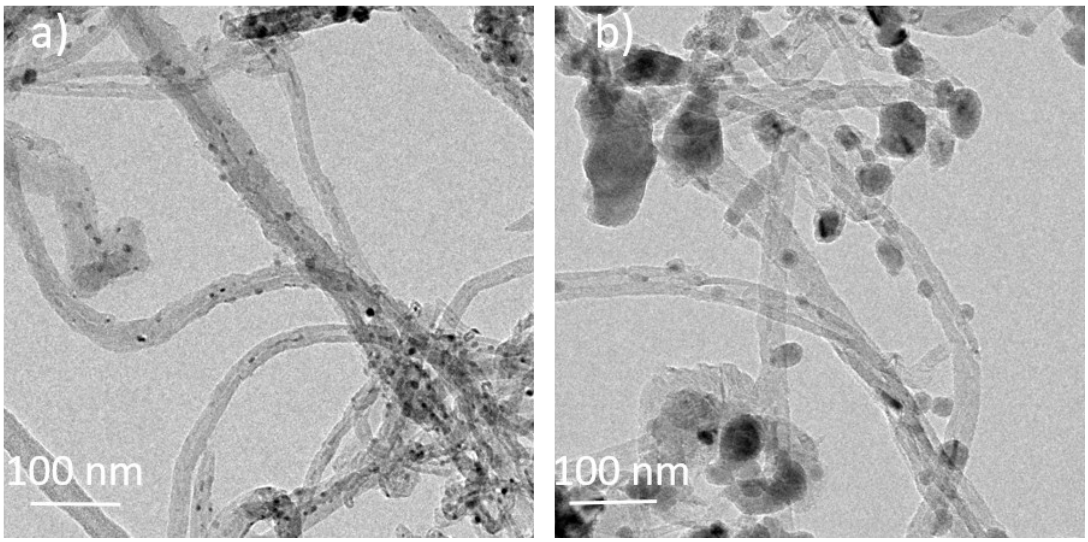

Fig. S1 The low-resolution TEM images of the prepared catalysts. a) NCNT/Ni-$NiMn_2O_4$, b) NCNT/Ni-$NiFe_2O_4$.

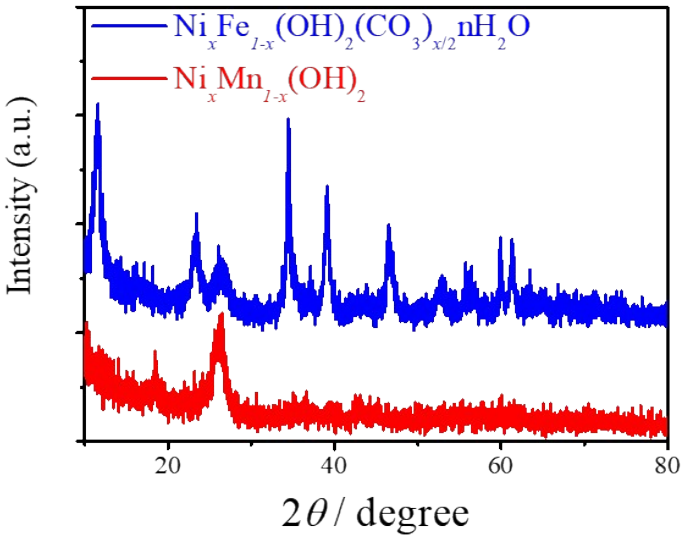

Fig. S2 The XRD patterns for the precursors of NCNT/Ni-$NiFe_2O_4$ and NCNT/Ni-$NiMn_2O_4$.

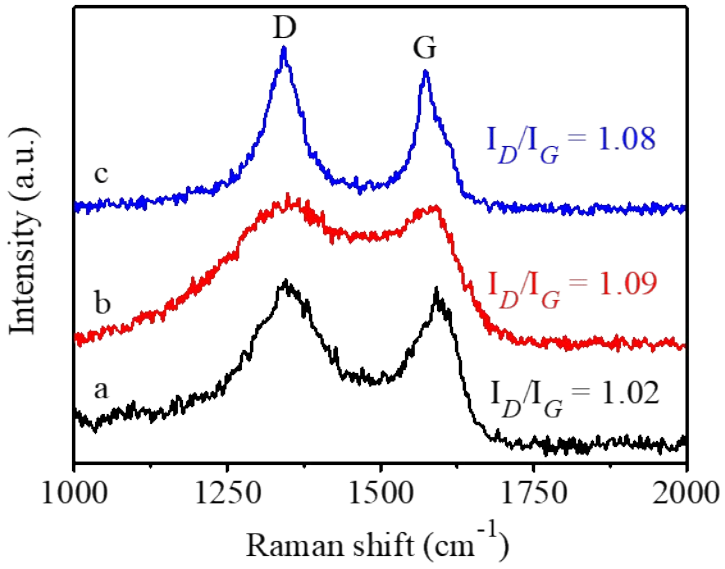

Fig. S3 Raman spectra of a) CNT, b) NCNT/Ni-$NiFe_2O_4$ and c) NCNT/Ni-$NiMn_2O_4$.

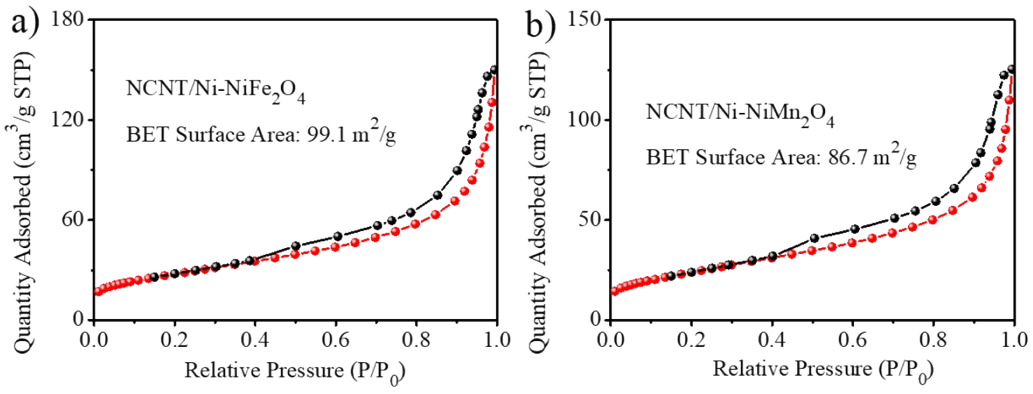

Fig. S4 Nitrogen adsorption-desorption isotherms of a) NCNT/Ni-$NiFe_2O_4$ and b) NCNT/Ni-$NiMn_2O_4$.

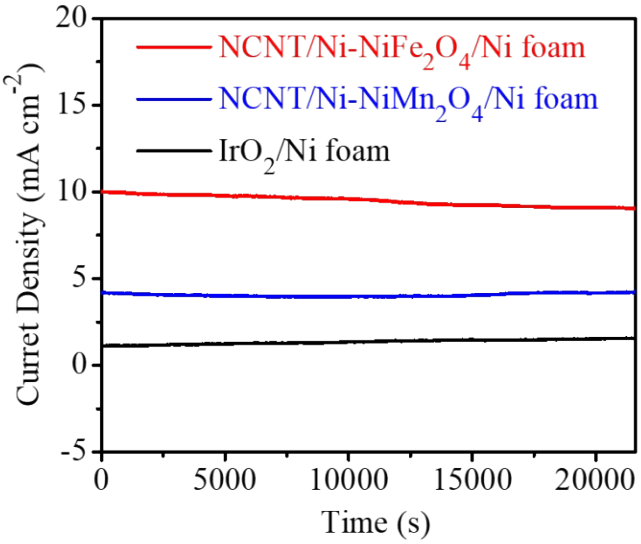

Fig. S5 Chronoamperometric responses of NCNT/Ni-$NiFe_2O_4$/Ni foam, NCNT/Ni-$NiMn_2O_4$/Ni foam and IrO_2/Ni foam for the OER at a constant potential of 1.48 V (*vs.* RHE).

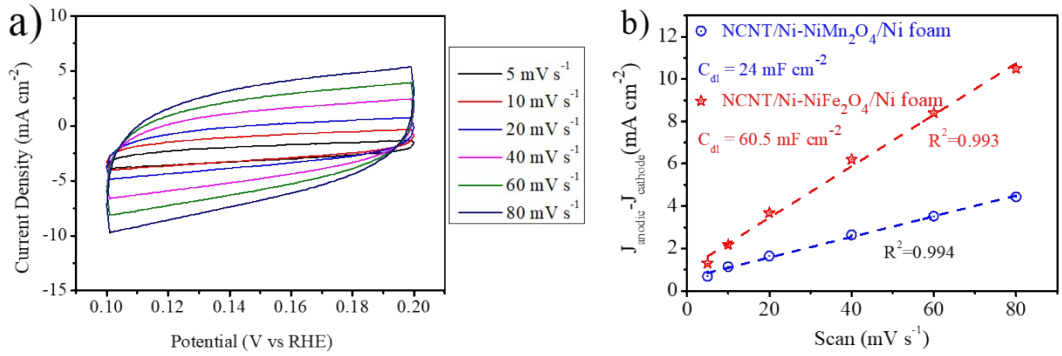

Fig. S6 a) Cyclic voltammograms recorded for a NCNT/Ni-$NiFe_2O_4$/Ni foam electrode in the approximate region of 0.1–0.2 V vs. RHE at various scan rates for the purpose of determining the double layer capacitance. b) Plot showing the extraction of the double-layer capacitance (C_{dl}) of NCNT/Ni-$NiFe_2O_4$/Ni foam and NCNT/Ni-$NiMn_2O_4$/Ni foam.

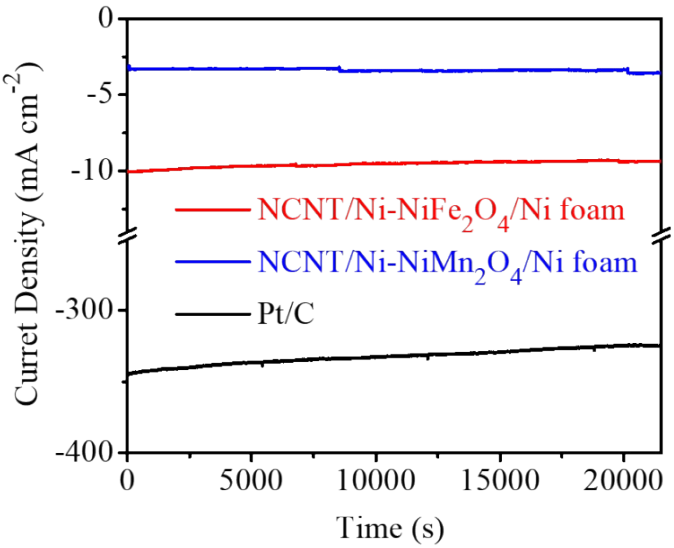

Fig. S7 Chronoamperometric responses of NCNT/Ni-$NiFe_2O_4$/Ni foam, NCNT/Ni-$NiMn_2O_4$/Ni foam and Pt/C for the HER at a constant potential of -0.14 V (*vs.* RHE).

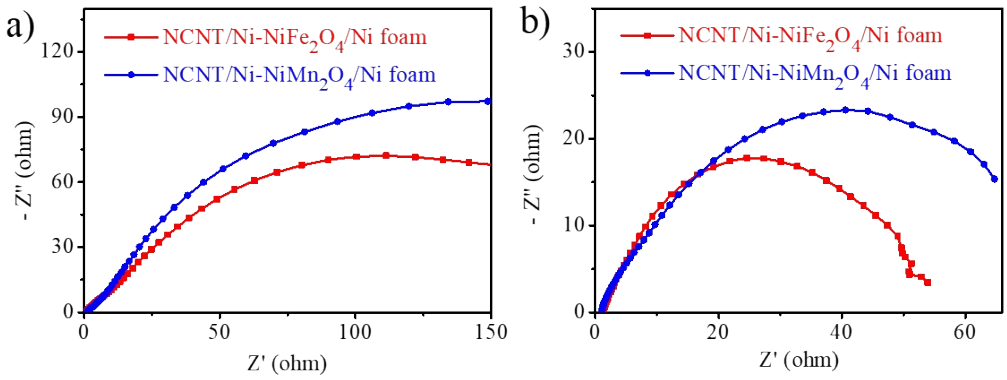

Fig. S8 Nyquist plots of NCNT/Ni-$NiFe_2O_4$/Ni foam and NCNT/Ni-$NiMn_2O_4$/Ni foam in 1 M KOH solution at open circuit potential: a) OER, b) HER.

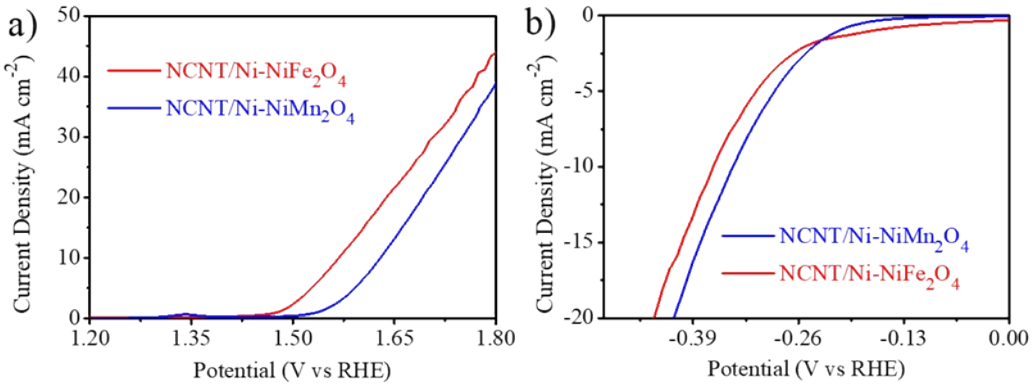

Fig. S9 a) Polarization curves of the NCNT/Ni-$NiFe_2O_4$ and NCNT/Ni-$NiMn_2O_4$ for OER in 1 M KOH electrolyte. b) Polarization curves of the NCNT/Ni-$NiFe_2O_4$ and NCNT/Ni-$NiMn_2O_4$ for HER in 1 M KOH electrolyte.

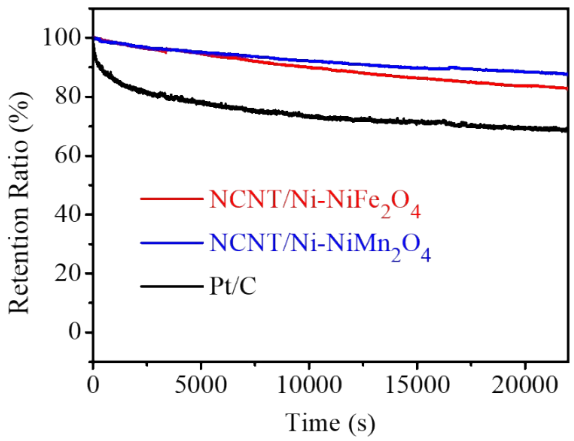

Fig. S10 Chronoamperometric curves of NCNT/Ni-$NiFe_2O_4$, NCNT/Ni-$NiMn_2O_4$, and Pt/C at 0.60 V versus RHE in O_2-saturated 0.1 M KOH electrolyte.

Table S1. Comparison of OER performance in alkaline medium for NCNT/Ni-$NiFe_2O_4$/Ni foam and NCNT/Ni-$NiMn_2O_4$/Ni foam with other OER electrocatalysts

Catalysts	Overpotential (mV) (@j=10 mA cm^{-2})	Tafel Slope (mV dec^{-1})	Ref.
NCNT/Ni-$NiFe_2O_4$/Ni foam	250	51	This work
NCNT/Ni-$NiMn_2O_4$/Ni foam	300	89	
CoP/CP	320	82.8	1
S-2-T5	302	90	2
Mo-MOFs-T5	407	93	
ZIF-67-T5	387	92	
RuO_2	355	104	
$Ni_{0.33}Co_{0.67}MoS_4$/CFC	283	68.8	3
Ir/C	345	107	4
Co–P film	390	91	
Co_9S_8	340	85.6	5
IrO_2	324	108	6
$Co_3(PO_4)_2$@N-C	317	62	7
$Mo_2C/Co_6Mo_6C_2$/NRGO	360	50	8
IrO_2	387	77	
Co_3ZnC/Co@CN	366	81	9
Co/$CNTs_{25\ wt\%}$	380	81	10
$Co_{0.8}Fe_{0.2}O_x$	430	85	
Fe_3O_4/$CNTs_{25\ wt\%}$	470	98	

Table S2. Comparison of HER performance in alkaline medium for NCNT/Ni-

$NiFe_2O_4$/Ni foam and NCNT/Ni-$NiMn_2O_4$/Ni foam with other HER electrocatalysts

Catalysts	Overpotential (mV)(@j = 10 mA cm^{-2})	Tafel Slope (mV dec^{-1})	Ref.
NCNT/Ni-$NiFe_2O_4$/Ni foam	140	85	This work
NCNT/Ni-$NiMn_2O_4$/Ni foam	188	76	
NiCo–$(MoO_4)^{2-}$/CFC	315	113.6	3
bare CFC	558	344.8	
CF	352	130	11
Ni/CF	400	167	
Ni_3S_2/NF	318	74	12
Cu_3P/CF (0.1 M KOH)	222	148	13
CF (0.1 M KOH)	521	184	
CoP/CC	209	129	14
Mo_2C/XC72	229	74.5	15
Mo_2C/C	165	63.6	
CoNi@NC	142	104	16
FeP NAs/CC	218	146	17
Cu_3P NW/CF	143	67	18
Co_2P nanorods	~152	171	19

Table S3. Comparison of ORR performance in alkaline medium for NCNT/Ni-$NiMn_2O_4$ with other ORR electrocatalysts

Catalysts	Catalyst Loading (mg cm^{-2})	Half-wave potential (V vs RHE)	Ref.
NCNT/Ni-$NiMn_2O_4$	0.208	0.71	This work
Au@Zn−Fe−C	71.5 μg_{Au} cm^{-2}	0.70	[20]
NGPC-800-5	0.102	0.55	[21]
NGPC-900-5	0.102	0.67	
NCNTs-20	0.570	0.62	[22]
N:C-MgNTA	0.153	0.75	[23]
AG	1.00	0.66	[24]
N-graphene	0.038	0.67	[25]
NG-800	0.034	0.68	[26]
HNCNSs-800	0.153	0.69	[27]
NG	0.04	0.71	[28]
N-CDs/G	0.05	0.71	[29]

References:

1. L. Ma, W. Zhang, P. Zhao, J. Liang, Y. Hu, G. Zhu, R. Chen, Z. Tie, J. Liu and Z. Jin, *J. Mater. Chem. A*, 2018, **6**, 20076-20082.
2. X. Shi, A. Wu, H. Yan, L. Zhang, C. Tian, L. Wang and H. Fu, *J. Mater. Chem. A*, 2018, **6**, 20100-20109.
3. L. Hang, T. Zhang, Y. Sun, D. Men, X. Lyu, Q. Zhang, W. Cai and Y. Li, *J. Mater. Chem. A*, 2018, **6**, 19555-19562.
4. S. Oh, H. Kim, Y. Kwon, M. Kim, E. Cho and H. Kwon, *J. Mater. Chem. A*, 2016, **4**, 18272-18277.
5. M. Al-Mamun, Y. Wang, P. Liu, Y. L. Zhong, H. Yin, X. Su, H. Zhang, H. Yang, D. Wang, Z. Tang and H. Zhao, *J. Mater. Chem. A*, 2016, **4**, 18314-18321.
6. S. Ma, Q. Zhu, L. Chen, W. Wang and D. Chen, *J. Mater. Chem. A*, 2016, **4**, 8149-8154.
7. C.-Z. Yuan, Y.-F. Jiang, Z. Wang, X. Xie, Z.-K. Yang, A. B. Yousaf and A.-W. Xu, *J. Mater. Chem. A*, 2016, **4**, 8155-8160.
8. C.-H. Liu, Y.-J. Tang, X.-L. Wang, W. Huang, S.-L. Li, L.-Z. Dong and Y.-Q. Lan, *J. Mater. Chem. A*, 2016, **4**, 18100-18106.
9. J. Su, G. Xia, R. Li, Y. Yang, J. Chen, R. Shi, P. Jiang and Q. Chen, *J. Mater. Chem. A*, 2016, **4**, 9204-9212.
10. Y. Fang, X. Li, S. Zhao, J. Wu, F. Li, M. Tian, X. Long, J. Jin and J. Ma, *RSC Adv.*, 2016, **6**, 80613-80620.
11. H. Yang, S. Luo, X. Li, S. Li, J. Jin and J. Ma, *J. Mater. Chem. A*, 2016, **4**, 18499-18508.
12. P. Ganesan, A. Sivanantham and S. Shanmugam, *J. Mater. Chem. A*, 2016, **4**, 16394-16402.
13. C. C. Hou, Q. Q. Chen, C. J. Wang, F. Liang, Z. Lin, W. F. Fu and Y. Chen, *ACS Appl. Mater. Interfaces*, 2016, **8**, 23037-23048.
14. J. Tian, Q. Liu, A. M. Asiri and X. Sun, *J. Am. Chem. Soc.*, 2014, **136**, 7587-7590.
15. M. Qamar, A. Adam, B. Merzougui, A. Helal, O. Abdulhamid and M. N. Siddiqui, *J. Mater. Chem. A*, 2016, **4**, 16225-16232.
16. J. Deng, P. Ren, D. Deng and X. Bao, *Angew. Chem. Int. Ed.*, 2015, **54**, 2100-2104.
17. Y. Liang, Q. Liu, A. M. Asiri, X. Sun and Y. Luo, *ACS Catal.*, 2014, **4**, 4065-4069.
18. J. Tian, Q. Liu, N. Cheng, A. M. Asiri and X. Sun, *Angew. Chem. Int. Ed.*, 2014, **53**, 9577-9581.
19. Z. Huang, Z. Chen, Z. Chen, C. Lv, M. G. Humphrey and C. Zhang, *Nano Energy*, 2014, **9**, 373-382.
20. J. Lu, W. Zhou, L. Wang, J. Jia, Y. Ke, L. Yang, K. Zhou, X. Liu, Z. Tang, L. Li and S. Chen, *ACS Catal.*, 2016, **6**, 1045-1053.
21. L. Zhang, Z. Su, F. Jiang, L. Yang, J. Qian, Y. Zhou, W. Li and M. Hong, *Nanoscale*, 2014, **6**, 6590-6602.
22. P. Su, H. Xiao, J. Zhao, Y. Yao, Z. Shao, C. Li and Q. Yang, *Chem. Sci.*, 2013, **4**, 2941.
23. D. Eisenberg, W. Stroek, N. J. Geels, C. S. Sandu, A. Heller, N. Yan and G. Rothenberg, *Chem.*, 2016, **22**, 501-505.
24. C. Zhang, R. Hao, H. Liao and Y. Hou, *Nano Energy*, 2013, **2**, 88-97.
25. Q. Liangti, L. Yong, B. Jong-Beom and D. J. A. N. Liming, *ACS Nano*, 2010, **4**, 1321-

1326.
26. A. Aijaz, N. Fujiwara and Q. Xu, *J. Am. Chem. Soc.*, 2014, **136**, 6790-6793.
27. L. Wang, S. Dou, J. Xu, H. K. Liu, S. Wang, J. Ma and S. X. Dou, *Chem. Commun.*, 2015, **51**, 11791-11794.
28. Z. H. Sheng, L. Shao, J. J. Chen, W. J. Bao, F. B. Wang and X. H. J. A. N. Xia, *ACS Nano*, 2011, **5**, 4350.
29. C. Hu, C. Yu, M. Li, X. Wang, Q. Dong, G. Wang and J. Qiu, *Chem. Commun.*, 2015, **51**, 3419-3422.